



ISSN: 0067-2904

Study of the Effect of Solar Indices on the Ionosphere Layer of Mars

Fahmi A. Mohammed*, Ahmed Ali Hameed

Department of Space Environment, Atmosphere and Space Science Center, Directorate of Space and Communications, Ministry of Science and Technology, Baghdad, Iraq

Received: 14/2/2022 Accepted: 13/11/2022 Published: 30/10/2023

Abstract

This paper studies the effect of the solar indices (total sunspot no., solar wind density and coronal mass ejection linear speed) on F_2 - layer electron density, as well as, the comparison of seasonal variations of electron density of F_2 - layer, N_mF_2 , for Mars at local noontime and for maximum and minimum solar cycles.

Results show that there is an inverse correlation between sunspot number, solar wind density, CME linear speed and ionosphere electron density for Mars, at maximum and minimum solar cycles. This correlation is clear when electron density is at minimum value.

The maximum value of N_mF_2 was in month 4 (Summer), month 21 (Winter) during maximum solar cycle, and month 1 (Spring), month 24 (Spring) during minimum solar cycle. The minimum value of N_mF_2 was in month 13 (Autumn) during maximum solar cycle, and month 9 (Summer) during minimum solar cycle. N_mF_2 was approximately constant in months 1- 8 (Spring and Summer) and gradually decreased in months 9- 13 (Summer and Autumn), then, gradually increased in months 14- 18 (Autumn and Winter) during maximum solar cycle (2012, 2013). In other hand, N_mF_2 was approximately constant in months 1- 5 (Spring and Summer) and gradually decreased in months 6- 9 (Summer), then, gradually increased in months 10- 16 (Autumn and Winter) during minimum solar cycle (2016, 2017).

Keywords: Solar coronal mass ejection, Solar wind density, Total sunspot number, F_2 - layer electron density, Maximum solar cycle, Minimum solar cycle.

دراسة تأثير المعاملات الشمسية على طبقة الايونوسفير لكوكب المريخ

فهمي عبد الرحمن محمد*, احمد علي حميد

قسم بيئة الفضاء، مركز علوم الجو و الفضاء، دائرة الفضاء و الاتصالات، وزارة العلوم و التكنولوجيا، بغداد، العراق.

الخلاصة

تم في هذا البحث دراسة التغيرات الفصلية في الكثافة الالكترونية لطبقة F_2 , N_mF_2 , لكوكب المريخ عند الظهر المحلي وللدورتين الشمسيتين العظمى والصغرى. تم ايضا دراسة تأثير تغير عدد البقع الشمسية الكلي، كثافة الرياح الشمسية والسرعة الخطية ل CME عليها.

بينت النتائج وجود علاقة عكسية بين كل من عدد البقع الشمسية، كثافة الرياح الشمسية، السرعة الخطية ل CME والكثافة الالكترونية الايونوسفيرية لكوكب المريخ عند الدورتين الشمسيتين العظمى والصغرى. وتكون العلاقة واضحة عندما تكون الكثافة الالكترونية في حدودها الدنيا.

*Email:fahmibeg@yahoo.com

اعلى قيمة ل $N_m F_2$ كانت في شهر 4 (فصل الصيف)، وشهر 21 (فصل الشتاء) خلال الدورة الشمسية العظمى، وشهر 1 (فصل الربيع) وشهر 24 (فصل الربيع) خلال الدورة الشمسية الصغرى. اقل قيمة ل $N_m F_2$ كانت في شهر 13 (فصل الخريف) خلال الدورة الشمسية العظمى، وفي شهر 9 (فصل الصيف) خلال الدورة الشمسية الصغرى.

تكون $N_m F_2$ ثابتة تقريبا في الاشهر 8 - 1 (فصلي الربيع والصيف) وتقل تدريجيا في الاشهر 13 - 9 (فصلي الصيف والخريف) ثم تزداد تدريجيا في الاشهر 18 - 14 (فصلي الخريف والشتاء) خلال الدورة الشمسية العظمى (2012, 2013). من ناحية اخرى تكون ثابتة تقريبا في الاشهر 5-1 (فصلي الربيع والصيف) وتقل تدريجيا في الاشهر 9-6 (فصل الصيف) ثم تزداد تدريجيا في الاشهر 16-10 (فصلي الخريف والشتاء) خلال الدورة الشمسية الصغرى (2016, 2017).

1. Introduction

The aim of this work is to investigate how the ionosphere of Mars affects radio waves propagation. The Martian ionosphere may be used as a reflector for global communication. This is crucial for future Mars ground-to-ground communication. The Martian dayside ionosphere has a critical frequency of ≈ 4.0 MHz for vertical incidence. This frequency is high enough to carry information, because the Martian ionosphere can effectively reflect these waves forward to areas beyond the line of sight. The stable condition in the dayside ionosphere also favors oblique incidence communication. However, because of low usable frequency and very unstable condition, the night side ionosphere has serious limitations for global communication [1].

An ionosphere is that region of the Martian atmosphere which is characterized by a weakly ionization (due to the greater distance from the Sun at Mars than Earth, the weaker solar radiation flux generates a lower plasma density in the Martian ionosphere). It is affected by the chemistry, dynamics and energetic of the neutral atmosphere.

It is considered the whole part of the edge between Mars and the solar wind, which continues from 100 to 210 km of the atmosphere, which plays an important role in determining the evolution of the climate and habitability of Mars over geological time, because it is involved in many atmospheric loss processes [2].

The ionosphere layer of Mars

The ionosphere layer of Mars consists originally of O_2^+ [3]. O^+ is the most plentiful ion at high altitudes under certain conditions (Mars General Circulation Model and Mars-Thermosphere General Circulation Model (MGCM- MTGCM)). Bearing species (such as NO^+), and metal species attained from meteoroids (such as M_g^+ and F_e^+), are important below an altitude of 100 km [4].

The Martian ionosphere splits into regions. A boundary called the Magnetic Pileup Boundary (MPB), which detaches solar wind plasma (H^+ , He^+) from Martian ions (O^+ , O_2^+), occurs near an altitude of 850 km on the dayside [5]. Another boundary, the Photo Electron Boundary (PEB), occurs near an altitude of 400 km. Ions of Martian origin lack peculiar peaks in their energy spectrum above the PEB. The topside ionosphere lies above an altitude of 200 km, where transport processes are important and the multiplicity of O and O^+ are relatively large [6]. Below this height, M2 layer exists, where the plasma densities are maximum over the entire ionosphere. Extreme Ultraviolet (EUV) photons emitted from the sun in the wavelength range (10 nm - 90 nm) are in charge of most of the ionization in the M2 layer and topside during the dayside. The M1 layer lies below the M2 layer by 20 Km. Since the flux of solar EUV photons is greatly absorbed here, therefore, X-rays (10 nm wavelength) are considered the

primary source of plasma in this layer [7]. Only (10- 20% of ions) in the M1 layer are produced directly by photo ionization, while most of them are produced by impact ionization due to photoelectrons and secondary electrons. Another plasma layer, the meteoric ion layer, exists near an altitude of 80 km and is believed to consist of atomic metal ions derived from ablating meteoroids [8].

The chemistry of the Martian ionosphere, dynamics as well as energetics, vary with both of position and time, because of the great variations in solar forcing, atmospheric dynamics, composition, and the magnetic field [9]. Therefore, knowledge of the Martian ionosphere is climacteric for evaluating the importance of atmospheric escape for the evolution of climate of the Mars. In general, understanding the Martian ionosphere is related to understanding Mars climate evolution.

At dayside, the electron densities in the Martian ionosphere are affected by the solar cycle, with electron densities increasing as ionizing solar radiation increases, and also, affected by the presence of magnetic fields, time of day, seasons, and the geographic location. Many researchers have tested changes of the peak electron density with different photographs of the ionizing solar radiation. (B., Sánchez- Cano, et al., 2016) [10] analyzed the response of the Martian ionosphere to solar activity, by taking into account variations in a range of parameters during four phases of the solar cycle throughout 2005– 2012. They concluded that the neutral scale height was different in each phase of the solar cycle, having a large variation with solar zenith angle during the moderate- ascending and high phases, while there was almost no variation during the moderate- descending and low phases. Between end- 2007 and end- 2009, an almost permanent absence of secondary layer resulted because of the low level of solar X-rays. Also, the ionosphere was more likely to be found in a more continuously magnetized state. The induced magnetic field from the solar wind, even if weak, could be strong enough to penetrate more than at other solar cycle phases.

(P., Withers, D., Morgan and D.A., Gurnett, 2014) [11] studied the variations in peak electron densities in the ionosphere of Mars over a full solar cycle. They used thousands of Mars Global Surveyor radio occultation measurements and hundreds of thousands of Mars Express topside radar sounder measurements from 1998 to 2013 to test whether the conclusions of previous workers withstand a substantial increase in the number of data points and near- continuous sampling across a range of ionizing solar irradiances. Data from narrow ranges in solar zenith angle (70° – 80°) and latitude (60°N – 80°N) were used in order to isolate, to the extent possible, the influence of irradiance. Ionospheric peak electron density increased smoothly with increasing F10.7, but this increase saturated at F10.7 values above 130 units. However, in contrast to some previous work, there was no change in behavior at an F10.7 value of 100 units. Saturation at high values of F10.7 also occurred in Earth's ionosphere and the underlying cause was that the appropriateness of F10.7 as a proxy for ionizing solar irradiance diminished at high solar activity. Similar overall trends were seen when the Lyman alpha emission or the Mg II core-to- wing index were used to replace F10.7 as a proxy for ionizing solar irradiance. Even when solar zenith angle and latitude were restricted, a time series of electron density residuals showed noteworthy trends. These trends might indicate a dependence of peak density on season, but they were not caused by changes in the Mars– Sun distance.

(F., González- Galindo, et al, 2020) [12] took advantage of the large ionospheric dataset collected by two instruments on Mars Express, the radar MARSIS on its Active Ionospheric Sounding (AIS) mode, and the radio- occultation experiment MaRS, during more than 16 years (and still running) of the mission. In order to isolate the seasonal variability, they removed the main variability factors, the change in the SZA and the change in the intrinsic solar activity, by using the well- known and thoroughly tested expressions derived from Chapman theory. Then

they averaged the obtained corrected peak electron densities and peak altitudes in bins of 5 degrees of Ls. Finally, they fitted a sinusoidal function to the obtained seasonal variability. The main obtained results were:

1. The seasonal variability of both the peak electron density and the peak altitude can be well reproduced by sinusoidal functions maximizing around the date of the perihelion. The fitted amplitudes were, for the peak electron density, about 9% of the annually- averaged value, and for the peak altitude about 9 km.
2. They found hints of latitudinal differences in the seasonal evolution. However, the large spread of the data did not allow for a detailed study of these latitudinal effects.
3. They did not find an increase in the peak electron density around Ls=30-70.

(M. J., Yao, et al., 2019) [13] investigated the structural variability of the Martian ionosphere with the aid of the radio occultation (RO) experiments made on board the recent Mars Atmosphere and Volatile Evolution (MAVEN) spacecraft. On the dayside, the RO electron density profiles were described by the superposition of two Chapman models, representing the contributions from both the primary layer and the low- altitude secondary layer. The inferred sub solar peak electron densities and altitudes were $1.24 \times 10^5 \text{ cm}^{-3}$ and 127 km for the former, and $4.28 \times 10^4 \text{ cm}^{-3}$ and 97 km for the latter, respectively, in general agreement with previous results appropriate for the low solar activity conditions. Our results strengthen the role of solar EUV and X- ray ionization as the driving source of plasma on the dayside of Mars. Beyond the terminator, a systematic decline in ionospheric total electron content is revealed by the MAVEN RO measurements made from the terminator crossing up to a solar zenith angle of 120° . Such a trend is indicative of day-to- night plasma transport as an important source for the night side Martian ionosphere.

(F., Duru, et al., 2019) [14] provided an overview of electron densities in the upper Martian ionosphere, obtained by investigating over 400,000 ionograms, during the course of about 11 years, corresponding to a full solar cycle. The data covered wide latitude and longitude ranges, 180° of solar zenith angle (SZA), and altitudes from about 250 to 1,550 km. The electron density profiles showed large fluctuations within each orbit and also for any given altitude and SZA range. However, the median electron density was almost constant on the dayside at a fixed altitude range, with the exception of a dip at around 30° SZA, at altitudes between 300 and 600 km. They observed a sudden drop in density as the terminator was approached from the dayside. For a fixed SZA range, the median electron density decreased exponentially with increasing altitude. The high- altitude scale height was composed of two exponential functions of SZA joined near the ionospheric terminator. Three- folding height changed between 45 and 214 km from the sub solar point up to 120° , corresponding to effective temperatures between about 165 and 780 K. Solar activity had a clear effect on the median electron densities above 500 km and one- folding height. The median electron density was higher during northern winters, as well as above regions of strong crustal fields on the dayside.

(B. M., Jakosky, et al., 2015) [15] studied the response of Mars to an interplanetary coronal mass ejection from MAVEN observations. To help understand ongoing ion loss to space, the Mars Atmosphere and Volatile Evolution (MAVEN) spacecraft made comprehensive measurements of the Mars upper atmosphere, ionosphere, and interactions with the Sun and solar wind during an interplanetary coronal mass ejection impact in March 2015. Responses included changes in the bow shock and magnetosheath, formation of widespread diffuse aurora, and enhancement of pick up ions. Observations and models both showed an enhancement in escape rate of ions to space during the event. Ion loss during solar events early in Mars history may have been a major contributor to the long- term evolution of the Mars atmosphere.

(B., Sánchez- Cano, et al., 2016) [16] observed that solar cycle variations in solar radiation created notable changes in the Martian ionosphere, which have been analyzed with Mars

Express plasma datasets. In general, lower densities and temperatures of the ionosphere were found during the low solar activity phase, while higher densities and temperatures were found during the high solar activity phase. In their paper, they assessed the degree of influence of the long term solar flux variations in the ionosphere of Mars.

(Z., Girazian and P., Withers, 2013) [17] showed that previous studies of the Mars ionosphere have concluded that increased solar flux led to increased peak electron densities. Many have described this relationship as $N_m \propto F^k$, where N_m is the peak electron density, F the ionizing flux, is represented by either F10.7 or E10.7, and k is an exponent. The derived exponents have varied greatly, but have a mean value of $k \approx 0.35$. They explored this relationship using solar spectra measurements from the TIMED-SEE instrument and Mars Global Surveyor radio occultation data. Derived exponents, $k \approx 0.50$, were larger than those found by previous studies that used F10.7 or E10.7 were close to the theoretical prediction of simplistic Chapman theory.

(M., Mendillo, et al., 2017) [18] showed that during the Mars Atmosphere and Volatile Evolution (MAVEN) mission's deep-dip #2 campaign of 17–22 April 2015, spacecraft instruments observed all of the physical parameters needed to assess the photo-chemical-equilibrium (PCE) explanation for ionospheric variability at a fixed altitude 135 km near the peak of the Martian ionosphere. MAVEN measurements of electron density, electron temperature, neutral CO₂ density, and solar irradiance were collected during 28 orbits. When inserted into the PCE equation, the measurements of varying PCE drivers correlated with the observed electron density variations to within instrumental uncertainty levels. The dominant source of this positive correlation was the variability of CO₂ densities associated with the longitudinal wave-2 component of non-migrating tides in the Martian thermosphere.

One of the most important models in determining Martian ionospheric electron density is the Mars Climate Database (MCD), which is defined as a database of meteorological fields derived from General Circulation Model (GCM) numerical simulations of the Martian atmosphere and validated using available observational data. For additional information about this model, return to the following references [19-24].

The structure of this work is as follows: Section 1 introduces the ionosphere of Mars, the interaction of radio waves with ionospheric plasma, and previous works. Section 2 explains the methodology, section 3 shows the results, section 4 highlights discussion, section 5 sums up the conclusions, and section 6 enlists the references.

2. Methodology

Data used in this paper were obtained, as illustrated in the following table:

Table 1: Websites of ionospheric and solar indices used in this paper

Ionospheric and solar indices	Abbreviation	Model and center	Website
Highest density of the F ₂ - layer	$N_m F_2$	Mars Climate Database (MCD)	http://www.mars.lmd.jussieu.fr

Linear Speed of Coronal Mass Ejection	CME	Solar and Heliospheric Observatory(SOHO)	https://cdaw.gsfc.nasa.gov/CME_list/
Solar wind density	SWD	Space Weather Prediction Center(SWPC), NOAA	https://www.swpc.noaa.gov/products/real-time-solar-wind
Total sunspot number	SN	Solar Influences Data analysis Center (SIDC)	http://www.sidc.oma.be

3. Results

Monthly averages of Mars N_mF_2 , total sunspot number, solar wind density (med.) and linear speed of CME at local noon time for 2012, 2013(maximum solar cycle), 2016, 2017(minimum solar cycle), were taken.

Figure 1 (A, B, C) illustrates variation of N_mF_2 for Mars (blue curve), with total sunspot no., solar wind density, CME linear speed respectively (red curve) during months of 2012, 2013.

Figure 2 (A, B, C) illustrates variation of N_mF_2 for Mars (blue curve), with total sunspot no., solar wind density, CME linear speed respectively (red curve) during months of 2016, 2017.

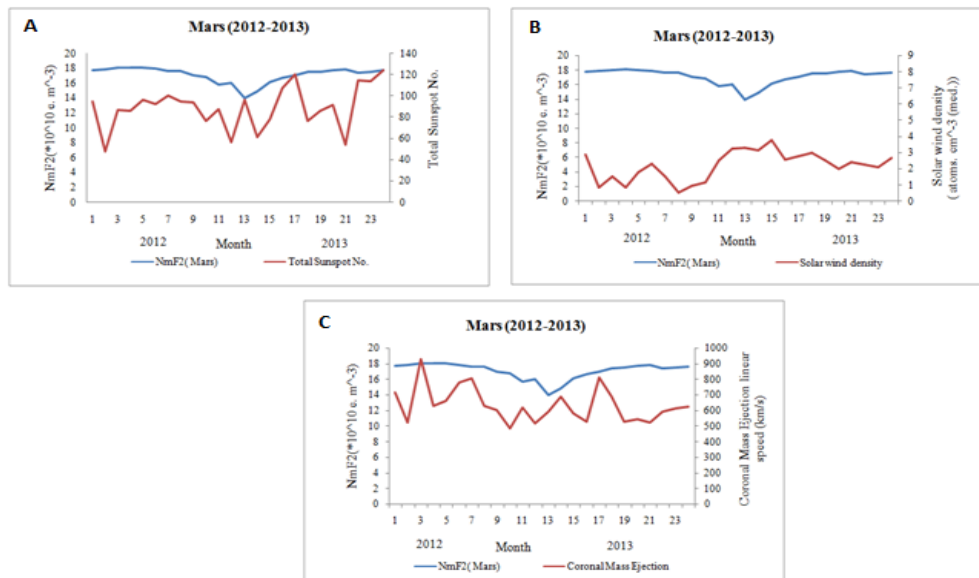


Figure 1: N_mF_2 for Mars Vs. (A) total sunspot no., (B) solar wind density and (C) coronal mass ejection linear speed at local noon time (**maximum solar cycle**).

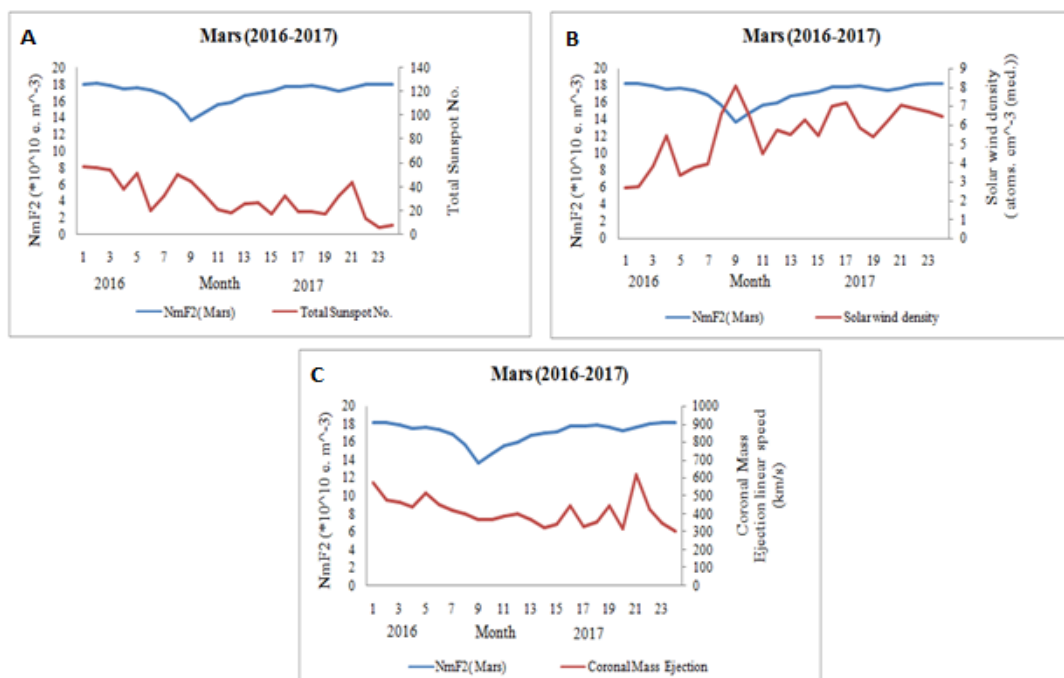


Figure 2: N_mF_2 for Mars Vs. (A) total sunspot no., (B) solar wind density and (C) coronal mass ejection linear speed at local noon time (**minimum solar cycle**).

4. Discussion

- Maximum solar cycle

It is observed from Figure 1(A, B, C) that the maximum value of N_mF_2 for Mars was $(18.1 \times 10^{10} \text{ m}^{-3})$ in month 4 (Summer) of 2012, then decreased to minimum value of $(14 \times 10^{10} \text{ m}^{-3})$ in month 13 (Autumn) of 2013 and increased gradually after that to maximum value of $(17.9 \times 10^{10} \text{ m}^{-3})$ in month 21 (Winter) of 2013.

According to the equation, $f_oF_2 = 9 \sqrt{N}$, maximum value of N_mF_2 $(18.1 \times 10^{10} \text{ m}^{-3})$ corresponds to maximum value of critical frequency, f_oF_2 (3.8 MHz). Minimum value of N_mF_2 $(14 \times 10^{10} \text{ m}^{-3})$ corresponds to minimum value of critical frequency, f_oF_2 (3.36 MHz). This will make Martian surface global communication possible.

It is observed from Figure 1(A) that the minimum value of total sunspot no. was (47.7) corresponded to maximum value of N_mF_2 $(17.86 \times 10^{10} \text{ m}^{-3})$ in month 2 (Spring) of 2012. The maximum value of it was (124.16) corresponded to maximum value of N_mF_2 $(17.7 \times 10^{10} \text{ m}^{-3})$ in month 24 (Spring) of 2013.

Minimum value of solar wind density was (0.53 cm^{-3}) corresponded to gradual decrease of N_mF_2 $(17.65 \times 10^{10} \text{ m}^{-3})$ in month 8 (Summer) of 2012, and maximum value of it was (3.76 cm^{-3}) corresponded to gradual increase of N_mF_2 $(16.16 \times 10^{10} \text{ m}^{-3})$ in month 15 (Autumn) of 2013, Figure 1(B).

Minimum value of CME linear speed was (485.6 km/s) corresponded to gradual decrease of N_mF_2 $(16.84 \times 10^{10} \text{ m}^{-3})$ in month 10 (Autumn) of 2012. Maximum value of it was (928.5 km/s) corresponded to gradual increase of N_mF_2 $(18.06 \times 10^{10} \text{ m}^{-3})$ in month 3 (Spring) of 2012, Figure 1(C).

- Minimum solar cycle

It is observed from Figure 2(A, B, C) that the maximum value of N_mF_2 for Mars was ($\approx 18.1 \times 10^{10} \text{ m}^{-3}$) in month 1 (Spring) of 2016, then decreased to minimum value of ($13.7 \times 10^{10} \text{ m}^{-3}$) in month 9 (Summer) of 2016 and increased gradually after that to a maximum value of ($\approx 18.1 \times 10^{10} \text{ m}^{-3}$) in month 24 (Spring) of 2017.

Maximum value of N_mF_2 ($18.1 \times 10^{10} \text{ m}^{-3}$) corresponded to maximum value of critical frequency, f_oF_2 (3.8 MHz). Minimum value of N_mF_2 ($13.7 \times 10^{10} \text{ m}^{-3}$) corresponded to minimum value of critical frequency, f_oF_2 (3.33 MHz). This will make Martian surface global communication possible.

It is observed from Figure 2(A) that the minimum value of total sunspot no. was (5.7) corresponded to maximum value of N_mF_2 ($18.1 \times 10^{10} \text{ m}^{-3}$) in month 23 (Spring) of 2017. The maximum value of it was (56.9) corresponded to a maximum value of N_mF_2 ($\approx 18.1 \times 10^{10} \text{ m}^{-3}$) in month 1 (Spring) of 2016.

Minimum value of solar wind density was (2.68 cm^{-3}) corresponded to a maximum value of N_mF_2 ($\approx 18.1 \times 10^{10} \text{ m}^{-3}$) in month 1 (Spring) of 2016, and maximum value of it was (8.08 cm^{-3}) corresponded to a minimum value of N_mF_2 ($13.7 \times 10^{10} \text{ m}^{-3}$) in month 9 (Summer) of 2016, Figure 2(B).

Minimum value of CME linear speed was (304.6 km/s) corresponded to a maximum value of N_mF_2 ($\approx 18.1 \times 10^{10} \text{ m}^{-3}$) in month 24 (Spring) of 2017. Maximum value of it was (619.68 km/s) corresponded to gradual increase of N_mF_2 ($17.66 \times 10^{10} \text{ m}^{-3}$) in month 21 (Winter) of 2017, Figure 2(C).

Shape of electron density variation curve during maximum solar cycle, is similar to it during minimum solar cycle; and this curve does not match during maximum solar cycle with it during minimum solar cycle; where it is crawling more during maximum solar cycle (as seen from Figures 1&2).

The difference between electron density values is small during maximum and minimum solar cycles (Figures 1&2).

Variation curve of sunspot no. values, is higher during maximum solar cycle than it is during minimum solar cycle.

Variation curve of solar wind density values, is higher during minimum solar cycle than it is during maximum solar cycle.

Variation curve of CME linear speed values, is higher during maximum solar cycle than it is during minimum solar cycle.

In this paper, results of N_mF_2 above Mars were inaccurate, because the height, h_mF_2 , for Mars was considered constant (120 Km) for all days of year whereas, in fact, this height varies from day to day. Years along complete solar cycle (11 years) were taken, to make the results more accurate.

5. Conclusions

An inverse correlation between sunspot number, solar wind density, CME linear speed and ionosphere electron density of Mars, at maximum and minimum solar cycles is found. This correlation is clear, when electron density is at minimum value (Figures 1 and 2).

6. Acknowledgements

We thank S. J. Bingham, S. R. Lewis, P. L. Read, Atmospheric, Oceanic & Planetary Physics, University of Oxford, UK, F. Forget, F. Hourdin, O. Talagrand, Y. Wanherdrick, M. Angelats I Coll, Laboratoire de Météorologie Dynamique du CNRS, Université Paris 6, Paris, France, M. Lopez- Valverde, M. Lopez- Puertas, Instituto de Astrofísica de Andalucía, Granada, Spain, J-P. Huot, European Space Research and Technology Centre, European Space Agency, Noordwijk, Netherlands, by preparing F₂- layer electron density data of Mars. We thank Dr. Nat Gopalswamy, by providing solar CME data. We thank the staff in Space Weather Prediction Center, NOAA, for supporting us with solar wind density data. Also, we thank Frédéric Clette, Royal Observatory of Belgium, Brussels, Belgium, by providing us with total sunspot number data.

7. References

- [1] C. Ho, N. Golshan, and A. Kliore, "Radio Wave Propagation Handbook for Communication on and Around Mars", *no. JPL-Publ-02-5*, 2002.
- [2] P. Withers, J. Espley, R. Lillis, D. Morgan, T. Cravens, J. Deighan, and O. Witasse, "The Ionosphere of Mars and its Importance for Climate Evolution", Community white paper submitted to the 2011 Planetary Science Decadal Survey, 2011.
- [3] C. A. Barth, A. I. Stewart, S. W. Bougher, D. M. Hunten, and S. J. Bauer, "Aeronomy of the Current Martian Atmosphere, in Mars", *University of Arizona Press, Tucson*, pp.1054- 1089, 1992.
- [4] T. L. McDunn, S. W. Bougher, J. Murphy, M. D. Smith, F. Forget, J. L. Bertaux, and F. Montmessin, "Simulating the Density and Thermal Structure of the Middle Atmosphere (~ 80 – 130 km) of Mars Using the MGCM- MTGCM: A Comparison with MEX/SPICAM Observations", *Icarus*, vol. 206, no. 5, 2010.
- [5] D.A. Gurnett, R.L. Huff, D.D. Morgan, A.M. Persoon, T.F. Averkamp, D.L. Kirchner, F. Duru, F. Akalin, A.J. Kopf, E. Nielsen, A. Safaeinili, J.J. Plaut, and G. Picardi, "An Overview of Radar Soundings of the Martian Ionosphere from the Mars Express Spacecraft", *Adv. Space Res.*, vol. 41, pp. 1335- 1346, 2008.
- [6] J. L., Fox, "Response of the Martian Thermosphere/Ionosphere to Enhanced Fluxes of Solar Soft X Rays", *J. Geophys. Res.*, vol. 109, no. A11310, 2004.
- [7] M. Mendillo, P. Withers, D. Hinson, H. Rishbeth, and B. Reinisch, "Effects of Solar Flares on the Ionosphere of Mars", *Science*, vol. 311, pp. 1135- 1138, 2006.
- [8] M. Patzold, S. Tellmann, B. Hausler, D. Hinson, R. Schaa, and G. L. Tyler, "A Sporadic Third Layer in the Ionosphere of Mars", *Science*, vol. 310, pp. 837- 839, 2005.
- [9] E. Chassefière and F. Leblanc, "Mars Atmospheric Escape and Evolution; Interaction with the Solar Wind", *Planet. Space Sci.*, vol. 52, no. 11, pp. 1039- 1058, 2004.
- [10] B. Sánchez- Cano, M. Lester, O. Witasse, S. E. Milan, B. E. S. Hall, M. Cartacci, K. Peter, D. D. Morgan, P. L. Blelly, S. Radicella, A. Cicchetti, R. Noschese, R. Orosei, and M. Pätzold, "Solar Cycle Variations in the Ionosphere of Mars as Seen by Multiple Mars Express Data Sets", *J. Geophys. Res. (Space Physics)*, vol. 121, pp. 2547– 2568, 2016. 121, 2547–2568, doi:10.1002/
- [11] P. Withers, D. Morgan and D.A. Gurnett, "Variations in Peak Electron Densities in the Ionosphere of Mars over a Full Solar Cycle", *Icarus*, vol. 251, pp. 5– 11, 2014.
- [12] F. González, D. Eusebio, F. Němec, K. Peter, A. Kopf, S. Tellman, and M. Pätzold, "Seasonal Variability of the Martian Dayside Ionosphere from Mars Express Observations", *Europlanet Science Congress 2020*, vol. 14, no. EPSC2020- 543, 2020.
- [13] M. J. Yao, J. Cui, X. S. Wu, Y. Y. Huang, and W. R. Wang, "Variability of the Martian Ionosphere from the MAVEN Radio Occultation Science Experiment", *Earth and Planetary Physics*, vol. 3, pp. 283– 289, 2019.
- [14] F. Duru, B. Brain, D. A. Gurnett, J. Halekas, D. D. Morgan, and C. J. Wilkinson, "Electron Density Profiles in the Upper Ionosphere of Mars from 11 Years of MARSIS Data: Variability Due to Seasons, Solar Cycle, and Crustal Magnetic Fields", *J. Geophys. Res. (Space physics)*, vol. 124, pp. 3057– 3066, 2019.

- [15] B.M.Jakosky, J.M. Grebowsky, J.G. Luhmann, J. Connerney, F. Eparvier, R. Ergun, J. Halekas, D. Larson, P. Mahaffy, and R. Yelle, "MAVEN Observations of the Response of Mars to an Interplanetary Coronal Mass Ejection", *Planetary Science*, vol. 350, no. 6261, 2015.
- [16] B. Sánchez- Cano, M. Lester, O. Witasse, P.L. Blelly, M. Cartacci, S.M. Radicella and M. Herraiz, "Solar Cycle Variations in the Ionosphere of Mars", *Física de la Tierra*, vol. 28, pp. 97- 110, 2016.
- [17] Z. Girazian and P. Withers, "The Dependence of Peak Electron Density in the Ionosphere of Mars on Solar Irradiance", *Geophys. Res. Lett.*, vol. 40, pp. 1960–1964, 2013.
- [18] M. Mendillo, C. Narvaez, M. F. Vogt, M. Mayyasi, J. Forbes, M. Galand, and L. Andersson, "Sources of Ionospheric Variability at Mars", *J. Geophys. Res. (Space Physics)*, vol. 122, pp. 9670– 9684, 2017.
- [19] M. Vals, F. Forget, E. Millour, A. Spiga, A. E. Maattanen, C. Wang, G. Gilli, V. Zakharov, D. Bardet, F. Montmessin, F. Lefèvre, F. Gonzalez-Galindo, and L. Montabone, "Toward a New Generation Mars Global Climate Model at LMD", *AGU, Fall Meeting 2018*, Dec. 2018, Washington, United States, 2018.
- [20] J. B. Madeleine, F. Forget, E. Millour, T. Navarro, and A. Spiga, "The Influence of Radiatively Active Water Ice Clouds on the Martian Climate", *Geophys. Res. Lett.*, vol. 39, no. L23202, 2012.
- [21] T. Navarro, J. B. Madeleine, F. Forget, A. Spiga, E. Millour, F. Montmessin, and A. Määttänen, "Modeling of the Martian Water Cycle with an Improved Representation of Water Ice Clouds", *European Planetary Science Congress 2013*, vol. 8, EPSC2013- 203, 2013.
- [22] F. González- Galindo, J. Y. Chaufray, M. A. López- Valverde, G. Gilli, F. Forget, F. Leblanc, R. Modolo, S. Hess, and M. Yagi, "Three- Dimensional Martian Ionosphere Model: I. The Photochemical Ionosphere below 180 km", *J. Geophys. Res. (Planets)*, vol. 118, pp. 2105– 2123, 2013.
- [23] F. González- Galindo, M. A. López-Valverde, F. Forget, M. García- Comas, E. Millour, and L. Montabone, "Variability of the Martian Thermosphere During Eight Martian Years as Simulated by a Ground- to- Exosphere Global Circulation Model", *J. Geophys. Res. (Planets)*, vol.120 (11), pp. 2020- 2035, 2015.
- [24] L. Montabone, F. Forget, E. Millour, R.J. Wilson, S.R. Lewis, B. Cantor, D. Kass, A. Kleinböhl, M.T. Lemmon, M.D. Smith, and M.J. Wolff, "Eight- Year Climatology of Dust Optical Depth on Mars", *Icarus*, vol. 251, pp. 65- 95, 2015.